Supplementary material for "Improved representation of phosphorus exchange on soil mineral surfaces reduces estimates of P limitation in temperate forest ecosystems"

Lin Yu[1,2], Silvia Caldararu[2], Bernhard Ahrens[2], Thomas Wutzler[2], Marion Schrumpf[2,3], Julian Helfenstein[4], Chiara Pistocchi[5], and Sönke Zaehle[2]

[1]Centre for Environmental and Climate Science, Lund University, Sölvegatan 37223 62 Lund, Sweden
[2]Max Planck Institute for Biogeochemistry, Hans-Knoell-Str. 10, Jena, 07745, Germany
[3]International Max Planck Research School (IMPRS) for Global Biogeochemical Cycles, Jena, 07745, Germany
[4]Agroscope, Reckenholzstrasse 191, 8046 Zürich, Switzerland
[5]Eco&Sols, Institut Agro, CIRAD, INRA, IRD, Place Viala 34060 Montpellier cedex 2, France

Correspondence to: Lin Yu (lin.yu@cec.lu.se)

S1 Additional figures and tables

Table S1: The normalized root mean square ratio (K_{nrmsr}) between simulated and observed soil properties along soil profiles of four models at five study sites (Fig. 2).

Soil properties	Site	4pool	siLang	dbLang	Control
SOC	BBR	0.32	0.32	0.32	0.32
	MTF	0.59	0.58	0.59	0.59
	VES	0.56	0.54	0.56	0.56
	COM	0.47	0.49	0.47	0.47
	LUE	0.59	0.58	0.63	0.61
SOM CN ratio	BBR	0.9	0.90	0.90	0.90
	MTF	0.95	0.95	0.95	0.95
	VES	0.93	0.93	0.93	0.93
	COM	0.85	0.84	0.85	0.85
	LUE	0.84	0.84	0.85	0.86
SOM CP ratio	BBR	0.54	0.54	0.54	0.54
	MTF	0.58	0.58	0.58	0.58
	VES	0.74	0.74	0.74	0.74
	COM	0.76	0.73	0.76	0.76
	LUE	0.61	0.61	0.63	0.67
Bulk density	BBR	0.69	0.69	0.69	0.69

	MTF	0.76	0.76	0.76	0.76
	VES	0.79	0.79	0.79	0.79
	COM	0.66	0.61	0.66	0.66
	LUE	0.81	0.81	0.82	0.84
SOP	BBR	0.33	0.33	0.33	0.33
	MTF	0.39	0.40	0.39	0.40
	VES	0.46	0.46	0.46	0.46
	COM	0.49	0.52	0.49	0.49
	LUE	0.49	0.50	0.45	0.42
SIP	BBR	0.77	0.78	0.77	0.79
	MTF	0.85	0.78	0.85	0.81
	VES	0.78	0.72	0.81	0.78
	COM	0.76	0.68	0.80	0.82
	LUE	0.81	0.81	0.81	0.77
Labile Pi	BBR	0.26	0.48	0.57	0.74
	MTF	0.29	0.47	0.68	0.71
	VES	0.3	0.51	0.60	0.56
	COM	0.18	0.37	0.36	0.76
	LUE	0.28	0.65	0.41	0.68
Sorbed Pi	BBR	NA	0.69	0.56	0.82
	MTF	NA	0.62	0.71	0.79
	VES	NA	0.55	0.78	0.72
	COM	NA	0.39	0.63	0.82
	LUE	NA	0.34	0.40	0.71
Lab-to-Exchangeable P	BBR	NA	0.47	0.62	0.80
	MTF	NA	0.46	0.70	0.67
	VES	NA	0.54	0.71	0.47
	COM	NA	0.35	0.37	0.72
	LUE	NA	0.55	0.62	0.61

Table S2 Parameters for sensitivity analysis

Symbol	Description	Value	Unit	Reference
v_{max,PO_4}	Maximum plant P uptake rate	0.044	µmol P/mol C/s	Thum et al. 2019
$x_{SOM_{fast}^{N:P}}$	N:P ratio of fast SOM pool	31	mol/mol	Thum et al. 2019

$x_{SOM_{slow}^{N:P}}$	N:P ratio of slow SOM pool	11.07	mol/mol	Thum et al. 2019
μ_P	Microbial phosphorus-use efficiency	0.8	mol/mol	Thum et al. 2019
τ_{fast}	Turnover time of fast SOM pool	2	years	Thum et al. 2019
τ_{slow}	Turnover time of slow SOM pool	100	years	Thum et al. 2019
τ_{biomin}	Phosphorus biomineralization turnover time	5	years	Thum et al. 2019
k_{weath}	Weathering rate constant of mineral soil	8.16208	10^{-8} μmol P/m^3/s	Yang et al. 2014
k_{ocl}	Occlusion coefficient of sorbed PO4	3.86	10^{-13} s^{-1}	Yang et al. 2014
k_{ads}	PO_4 (ab)sorption rate from P_{lab} to P_{sorb}	651.852	μmol P/kg soil/s	Yang et al. 2014
k_{des}	PO_4 desorption rate from P_{sorb} to P_{lab}	733	μmol P/kg soil/s	Yang et al. 2014
K_{m,PO_4}^{pH}	Correction coefficient of pH on Langmuir Km	0.4	–	this study
$Q_{max,PO_4}^{Al/Fe}$	Phosphate sorption capacity of Al/Fe oxides	9.134	mmol P/kg clay	this study
Q_{max,PO_4}^{fs}	Phosphate sorption capacity of fine soil	9.134	mmol P/kg fine soil	this study
Q_{max,PO_4}^{sand}	Phosphate sorption capacity of sand	4.567	mmol P/kg sand	this study
Q_{max,PO_4}^{OM}	Phosphate sorption capacity of organic matter	4.567	mmol P/kg OM	this study

Table S3. The weighted mean values of partial correlation coefficient against all the output variables (Fig. 5) for the 16 selected parameters (Table S2) in the LHS sensitivity runs. Overall importance of parameters is measured by first calculating the RPCC for each output variable and then calculating the mean of the absolute RPCC values across selected outputs in Fig.5, weighted by the uncertainty contribution of these model outputs

Models, sites & Parameters	dbLang		siLang	
	COM	MTF	COM	MTF
τ_{slow}	0.89	0.97	0.82	0.78
τ_{fast}	0.55	0.61	0.34	0.35
$x_{SOM_{slow}^{N:P}}$	0.63	0.34	0.62	0.32

k_{des}	0.03	0.03	0.61	0.54
k_{ads}	0.02	0.02	0.90	0.86
v_{max,PO_4}	0.31	0.17	0.50	0.39
$x_{SOM_{fast}^{N:P}}$	0.28	0.22	0.26	0.26
Q_{max,PO_4}^{sand}	0.14	0.16	0.21	0.19
Q_{max,PO_4}^{fs}	0.20	0.26	0.56	0.28
$Q_{max,PO_4}^{Al/Fe}$	0.32	0.32	0.05	0.18
Q_{max,PO_4}^{OM}	0.14	0.12	0.10	0.18
K_{m,PO_4}^{pH}	0.24	0.23	0.21	0.14
k_{weath}	0.25	0.13	0.31	0.10
τ_{biomin}	0.03	0.02	0.02	0.01
k_{ocl}	0.04	0.04	0.03	0.03
μ_P	0.02	0.01	0.01	0.01

Figure S1: Reported Smax, Km, and Ptot in batch experiment data. The plot is produced based on 258 data inputs from [1-27]. The processing details are given in Section "A1 Processing of the reviewed data".

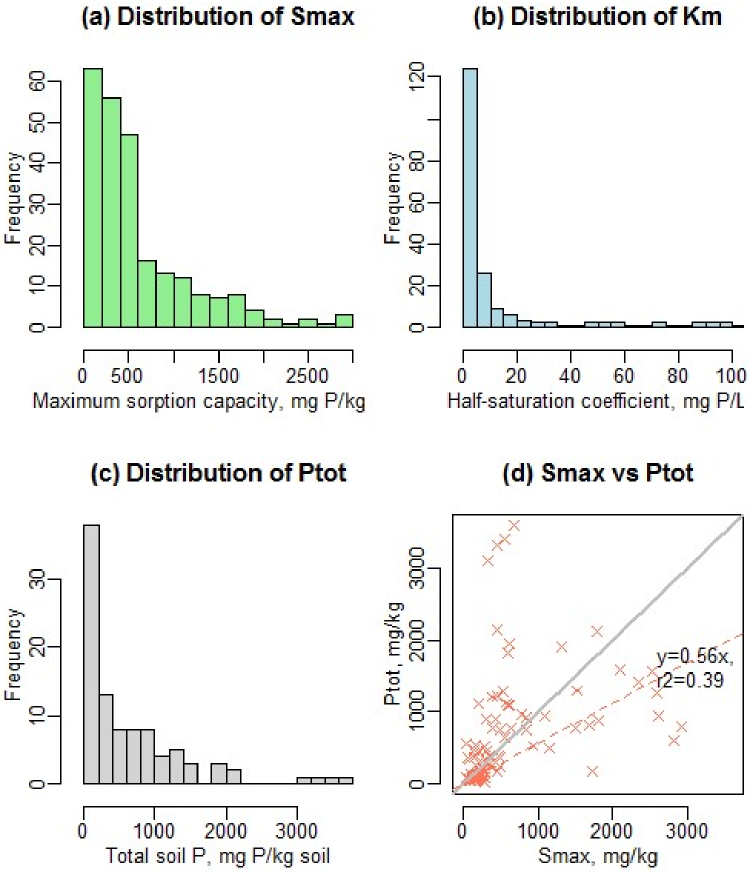

Figure S2: Figure 4 Simulated GPP, LAI, aboveground C, fine root C, plant uptakes of N and P

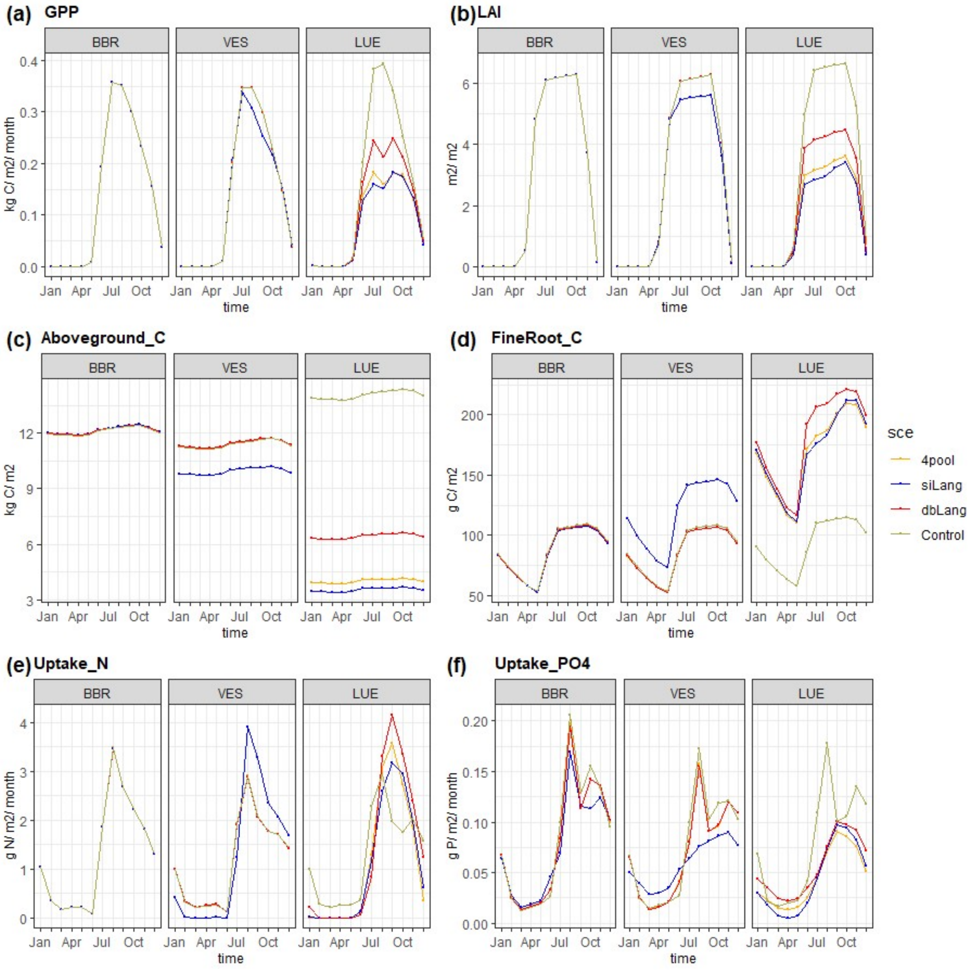

Figure S3: 4pool model responses to C and P fertilisation

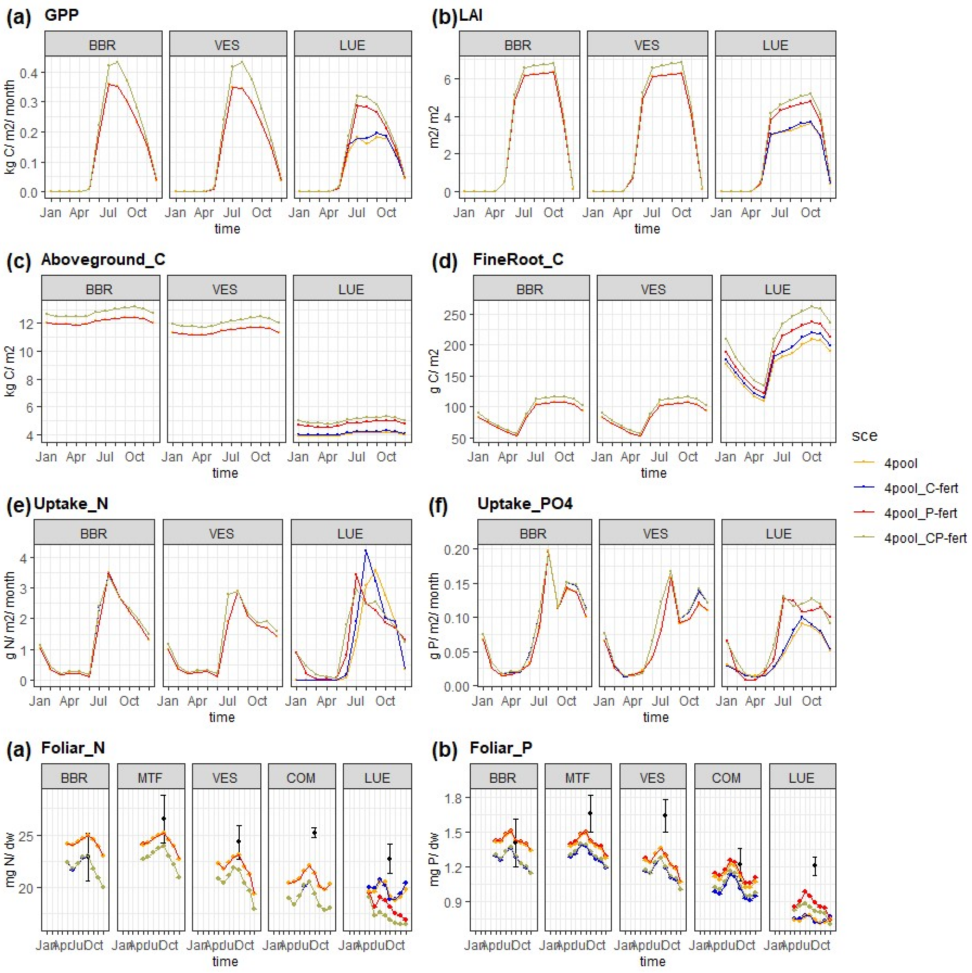

Figure S4: dbLang model responses to C and P fertilization

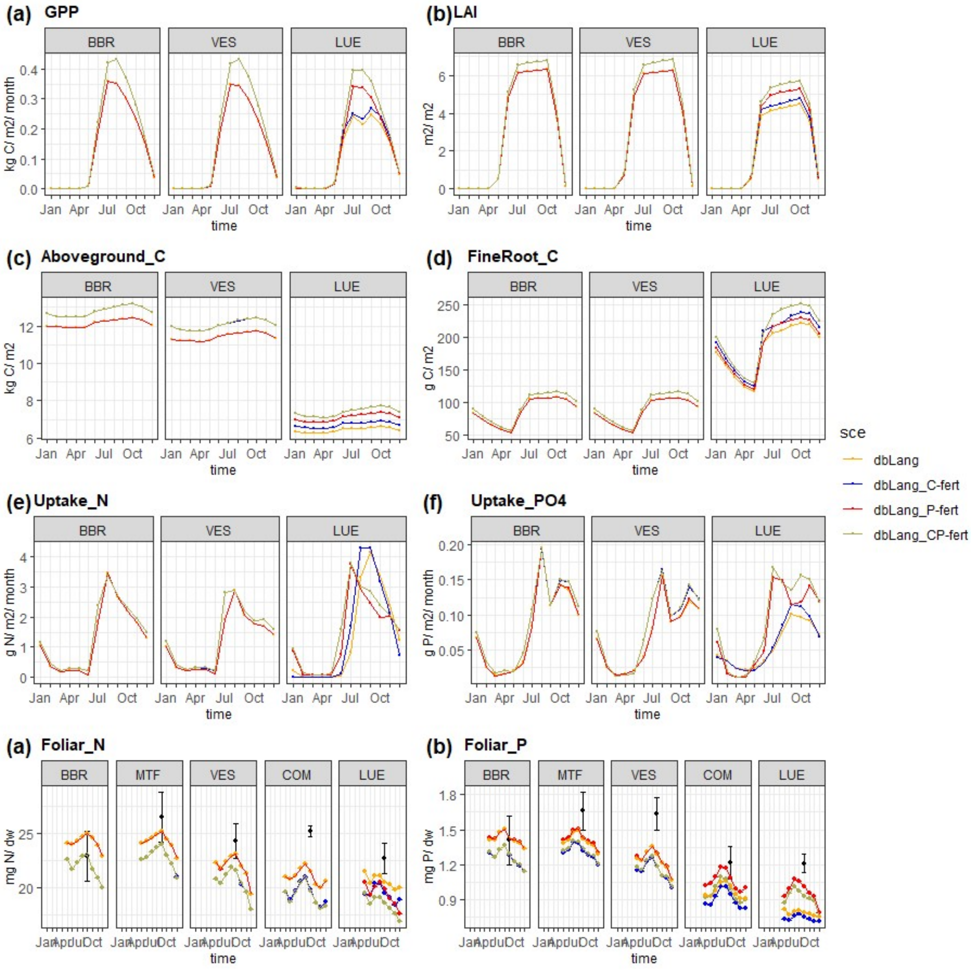

Figure S5: siLang model responses to C and P fertilization

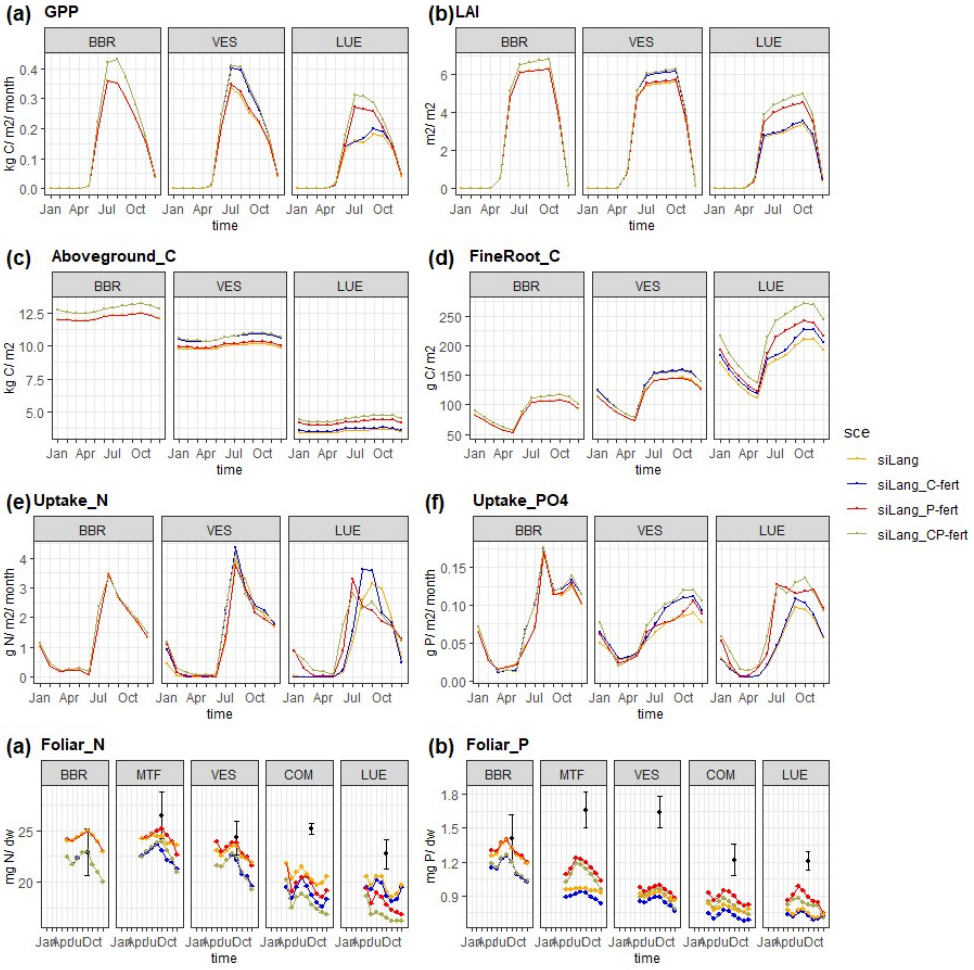

Figure S6: Normalized output variations in the LHS sensitivity analysis of siLang and dbLang models at COM and MTF sites. The selected output variables include GPP (kg C/m^2/yr), foliar N content (mg N/g d.w.), foliar P content (mg P/g d.w.), plant C (kg C/m^2), SOC stock (kg C/m^2), SOP and SIP stocks (g P/m^2) and Lab-to-Exchangeable P ratio. All the calculations are performed based on data from the last 10 years of 1000 LHS simulations, and soil variables are based on the topmost 1m of soil. The numbers below bars are the mean values of the 1000 LHS runs, and bars are the distribution of all 1000 LHS runs normalized to the mean value.

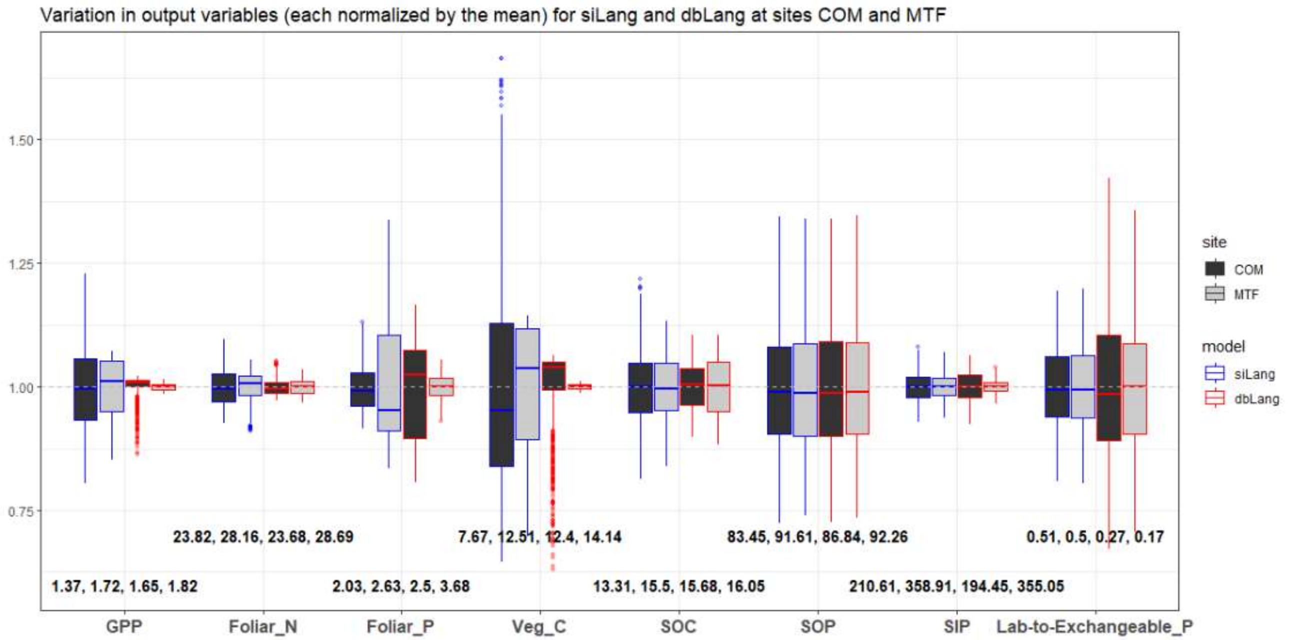

The simulated annual GPP was lower in **siLang** (1.37±0.12 and 1.72±0.12 kg C/m^2/yr for COM and MTF) than in **dbLang** (1.65±0.04 and 1.82±0.01 kg C/m^2/yr for COM and MTF), and **siLang** responded more strongly to changes of P cycling processes parameterization than **dbLang** (Figs. 5 and S6), reflecting a stronger P-control on plant productivity in the **siLang** model. This stronger P limitation also led to lower plant and soil C in **siLang** (plant C: 7.67±1.58 and 12.51±1.55 kg C/m^2 for COM and MTF; soil C: 13.31±0.94 and 15.50±0.96 kg C/m^2 for COM and MTF) than in **dbLang** (plant C: 12.40±1.06 and 14.14±0.07 kg C/m^2 for COM and MTF; soil C: 15.78±0.76 and 16.04±0.95 kg C/m^2 for COM and MTF).

Figure S7: Responses of Labile-to-Active P fraction to changes in parameterization in siLang and dbLang models at COM and MTF sites

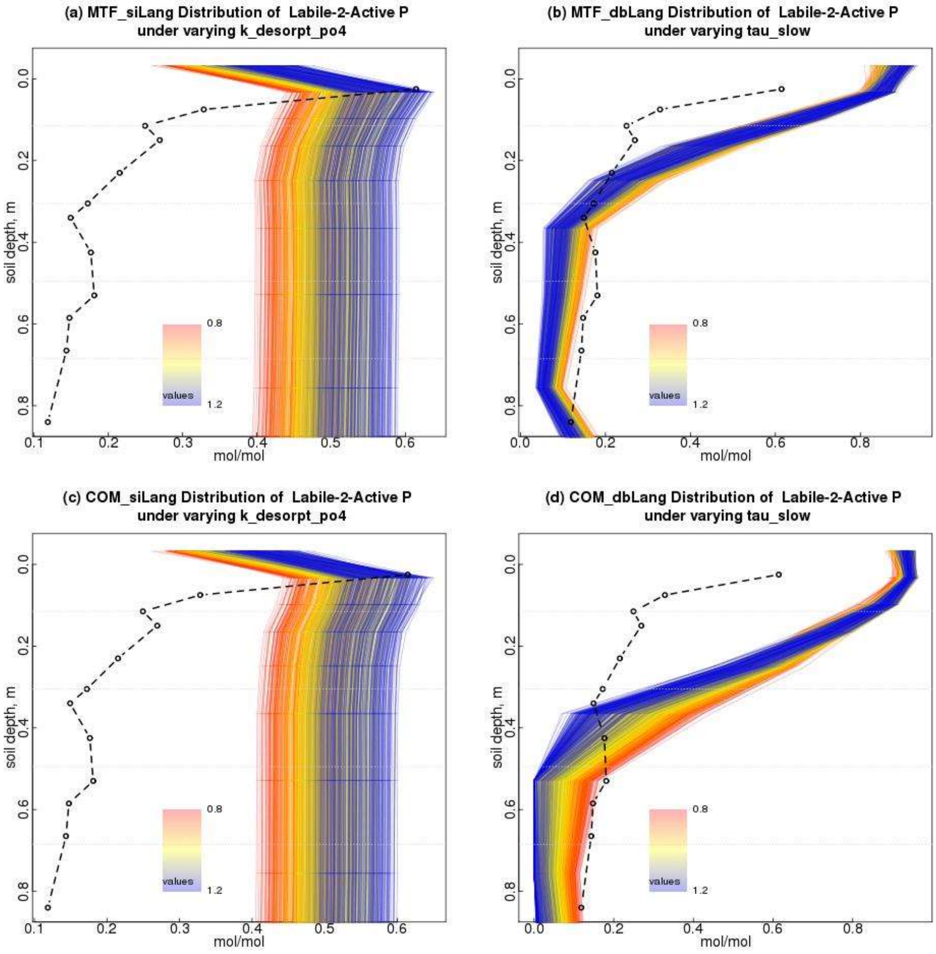

S2 Processing of the reviewed data

As most P species present in soil solution are negatively charged, the major P sorbents are those constituents that bear positive charges. These include hydroxyl (Fe and Al oxides), carboxyl (organic matter) or silanol (clays) groups [28]. Of the studies that we reviewed, the P sorption capacity of soils has been variously related to soil pH [18, 23, 29], mineralogy or clay content [30-32], organic complexes of Fe and Al [33], soil organic matter such as DOC, organic acids, DOP etc. [29, 34-37], calcium carbonate [8, 26], soil pedogenesis [32, 35], extractable Fe and Al oxides, hydroxides, and oxyhydroxides, and other soil properties. The correlation between soil properties and Langmuir parameters are demonstrated in the figure below,

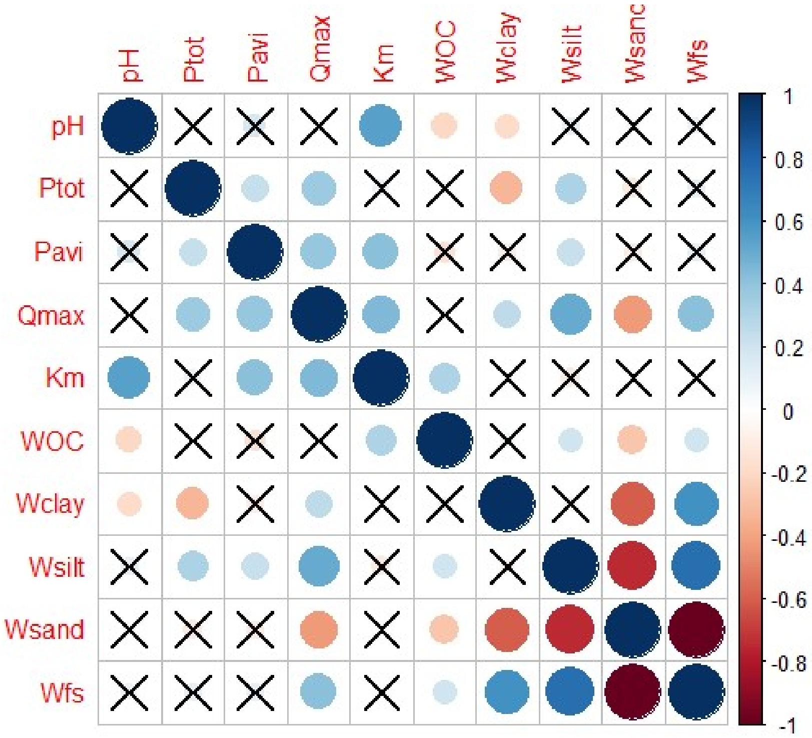

Figure S8: Correlation between reported soil properties and Langmuir parameters from reviewed literature. More details given below.

To derive Figs. S1 and S8, the raw data from reference [1-27] were processed in the following steps:

1. Conversion of Langmuir coefficient from K_L to K_m. The Langmuir isotherm in the batch sorption experiments were reporting the Langmuir coefficient either as K_L in the unit of L/mg P, or as K_m in the unit of mg P/L. We unified the Langmuir coefficient to K_m by inverting 1/ K_L. To further generate the data for Table 1 and Fig. 2, we assumed that the soil water content for all experiments data are 330 L/m^3 soil and converted the unit from mg P/L to g P/m^2.
2. Selection of reported soil properties. The reviewed papers don't follow the same protocols in reporting the soil properties, apart from the two Langmuir isotherm parameters (S_{max} and K_m), many studies also reported organic matter contents (OM, in percent), soil texture (clay, silt and sand), pH (measured in water or $CaCl_2$/KCl), total soil P (Ptot, mg P/ kg soil), available P (Pavi, mg P/kg soil). We selected the abovementioned variables (pH as water measured values) to understand their relationships with Langmuir parameters.

Conversion of OM and soil texture to weights. In order to derive a weight-based relationship between Langmuir parameters, the reported OM contents and soil texture were converted to OM and clay, silt, sand weights, assuming an OM density of 250 kg/m^3 and mineral soil bulk density of 1000 kg/m^3. The correlation between the soil properties and Langmuir parameters are plotted in Fig. S7, where WOC, Wclay, Wsilt, Wsand are the OM, clay, silt, and sand weights [kg/m^3], respectively, and Wfs stands for weight of fine soil (clay plus silt).

S3 Double-surface Langmuir isotherm and parametrization

As both single- and double-surface Langmuir isotherm could be fitted against the same experiments data, the apparent maximum sorption capacity (S_{max}) in Eq. 1 is the sum of sorption maxima of two sorption sites ($S_{max,1}$ and $S_{max,2}$, Eqs. 3.1 and 3.2) and the apparent Langmuir coefficient (K_m) in Eq. 1 could be derived mathematically from the Langmuir coefficients of two sorption sites ($K_{m,1}$ and $K_{m,2}$, Eqs. 3.4 and 3.5).

Following the concept of double-surface Langmuir isotherm, we assume that the apparent maximum sorption capacity and Langmuir coefficient in all the batch sorption experiment are in fact a combined value of two (or more) sorption surfaces.

$$S = S_{max}\frac{P_{sol}}{K_m+P_{sol}} = S_{max,1}\frac{P_{sol}}{K_{m,1}+P_{sol}} + S_{max,2}\frac{P_{sol}}{K_{m,2}+P_{sol}}, \tag{S1}$$

Where the apparent maximum sorption capacity is the sum of sorption maxima of individual sorption surface,

$$S_{max} = S_{max,1} + S_{max,2} \tag{S2}$$

The apparent Langmuir coefficient is calculated in Eq.3d which is derived using the differential form of double-surface Langmuir isotherm,

$$\frac{dS}{dt} = \frac{S_{max}K_m}{(K_m+P_{sol})^2}\frac{dP_{sol}}{dt} = \frac{S_{max,1}K_{m,1}}{\left(K_{m,1}+P_{sol}\right)^2}\frac{dP_{sol}}{dt} + \frac{S_{max,2}K_{m,2}}{\left(K_{m,2}+P_{sol}\right)^2}\frac{dP_{sol}}{dt}, \text{ thus} \tag{S3}$$

$$K_m = \frac{\frac{S_{max}}{hlp} - 2P_{sol} \pm \sqrt{\frac{{S_{max}}^2}{hl\ ^2} - 4\frac{S_{max}P_{sol}}{hlp}}}{2}, \text{ where} \tag{S3.1}$$

$$hlp = \frac{S_{max,1}K_{m,1}}{\left(K_{m,1}+P_{lab}\right)^2} + \frac{S_{max,2}K_{m,2}}{\left(K_{m,2}+P_{lab}\right)^2} \tag{S3.2}$$

To estimate the sorption maximum and Langmuir coefficient of each sorption surface, we derived pedo-functions based on the reported soil properties from the batch sorption experiment data. As shown in Fig.S2, the maximum sorption capacity is positively correlated with clay and silt content, negatively correlated with sand content and does not show correlation with OM content; the Langmuir coefficient is strongly correlated with soil pH and OM content and not correlated with soil texture. Given the high uncertainty in the original experiment data, and the lack of extractable Al and Fe content that represent crystalline and non-crystalline Fe and Al oxides and organic complexes of Fe and Al, which are commonly considered the main sorbents of P, we tested different combination of soil sorbents and finally used a four sorbents pedo-functions for S_{max} and K_m,

$$S_{max} = S_{max,1} + S_{max,2} \tag{Equation S2}$$

$$S_{max,1} = Q_{max,PO_4}^{Al/Fe} \cdot W_{clay} \cdot f_{Al/Fe} + Q_{max,PO_4}^{OM} \cdot W_{OM} \tag{Equation S4.1}$$

$$S_{max,2} = Q_{max,PO_4}^{fs} \cdot W_{clay+silt} \cdot f_{Al/Fe} + Q_{max,PO_4}^{sand} \cdot W_{sand} \tag{Equation S4.2}$$

$$f_{Al/Fe} = \frac{(Fe_{ox}+Al_{ox})}{10mmol/kg} \tag{Equation S4.3}$$

$$K_{m,1} = k_{ph} \cdot pH \cdot f\left(K_m^{OM}, K_m^{Al/Fe}\right) \tag{Equation S4.4}$$

$$K_{m,2} = k_{ph} \cdot pH \cdot f\left(K_m^{fs}, K_m^{sand}\right) \tag{Equation S4.5}$$

Where $Q^{Al/Fe}_{max,PO_4}$ is the sorption capacity of crystalline and non-crystalline Fe and Al oxides normalized by the clay content; $f_{Al/Fe}$ is the correction coefficient of oxalate-extractable Al and Fe, which is calculated in Eq. 4.3, assuming that most Al- & Fe- (hydro)oxides reside in clay and the rest in silt; k_{ph} is a unitless correction factor to account for the effect of pH, and $K_{m,1}$ and $K_{m,2}$ are calculated using Eqs.4.4 and 4.5.

Table S4: Parameters for double-surface Langmuir isotherm

Symbol	Description	Value	Unit
K^{pH}_{m,PO_4}	Correction coefficient of pH on Langmuir Km	0.4	–
$Q^{Al/Fe}_{max,PO_4}$	Phosphate sorption capacity of Al/Fe oxides	9.134	mmol P/kg clay
Q^{fs}_{max,PO_4}	Phosphate sorption capacity of fine soil	9.134	mmol P/kg fine soil
Q^{sand}_{max,PO_4}	Phosphate sorption capacity of sand	4.567	mmol P/kg sand
Q^{OM}_{max,PO_4}	Phosphate sorption capacity of organic matter	4.567	mmol P/kg OM
$K^{Al/Fe}_{m}$	Langmuir coefficient of Al/Fe oxides	315.445	µmol P/L
K^{fs}_{m}	Langmuir coefficient of fine soil	2.176	mmol P/L
K^{OM}_{m}	Langmuir coefficient of soil organic matter	20	mmol P/L
K^{sand}_{m}	Langmuir coefficient of sand	20	mmol P/L

S4 Deep soil inorganic P initialization

The initial inorganic P pools of soils deeper than 1m was calculated using the following equations:

$$P^{frac}_{primary} = min\left(\frac{2*\sqrt{z},\ 3.4}{3.5}\right) \qquad \text{(Equation S5.1)}$$

$$P^{frac}_{exchangabl} = \frac{0.8^{2*z}}{3.5} \qquad \text{(Equation S5.2)}$$

$$P^{frac}_{ocl} = max\left(1 - P^{frac}_{primary} - P^{frac}_{exchangabl}\ ,\ \frac{0.1}{3.5}\right) \qquad \text{(Equation S5.3)}$$

Where z is the soil depth in m, and $P_{exchangeable}$ includes P_{sorb} and P_{lab} with a constant ratio of 9/8 at all depths. The total soil inorganic P contents for all the study sites (g P/m^3, >1m depth) are given in Table S5.

depth (m)	BBR	MTF	VES	COM	LUE
1.14	124.1	12.9	31.0	18.8	7.6

1.58	133.9	15.0	32.8	18.3	5.8
2.20	100.0	16.7	40.7	23.4	5.9
3.06	126.0	16.9	41.9	25.0	6.8
4.27	122.2	17.5	41.1	21.1	8.3
5.95	145.0	15.1	48.4	21.9	8.4
8.22	90.0	15.6	54.0	15.1	8.5

Table S5: The total soil inorganic P contents (g P/m^3, >1m depth) for all study sites at specific depth at QUINCY initialization. The initial values of soil inorganic P contents at top 1 m soil were prescribed from the Hedley fractionation measurements.

1. Abekoe, M.K. and K.L. Sahrawat, *Phosphate retention and extractability in soils of the humid zone in West Africa.* Geoderma, 2001. **102**(1-2): p. 175-187.

2. Ahmed, M.F., et al., *Phosphorus adsorption in some Australian soils and influence of bacteria on the desorption of phosphorus.* Communications in Soil Science and Plant Analysis, 2008. **39**(9-10): p. 1269-1294.

3. Chakraborty, D., V.D. Nair, and W.G. Harris, *Compositional Differences Between Alaquods and Paleudults Affecting Phosphorus Sorption-Desorption Behavior.* Soil Science, 2012. **177**(3): p. 188-197.

4. Debicka, M., et al., *Organic matter effects on phosphorus sorption in sandy soils.* Archives of Agronomy and Soil Science, 2015. **62**(6): p. 840-855.

5. Dossa, E.L., et al., *Phosphorus Sorption and Desorption in Semiarid Soils of Senegal Amended With Native Shrub Residues.* Soil Science, 2008. **173**(10): p. 669-682.

6. Fan, H., et al., *Effects of freeze–thaw cycles on phosphorus adsorption and desorption in the black soil of northeastern China.* Acta Agriculturae Scandinavica, Section B — Soil & Plant Science, 2014. **64**(1): p. 24-32.

7. Guedes, R.S., et al., *Adsorption and desorption kinetics and phosphorus hysteresis in highly weathered soil by stirred flow chamber experiments.* Soil and Tillage Research, 2016. **162**: p. 46-54.

8. Harrell, D.L. and J.J. Wang, *Fractionation and Sorption of Inorganic Phosphorus in Louisiana Calcareous Soils.* Soil Science, 2006. **171**(1): p. 39-51.

9. Hartono, A., S. Funakawa, and T. Kosaki, *Phosphorus sorption-desorption characteristics of selected acid upland soils in Indonesia.* Soil Science and Plant Nutrition, 2005. **51**(6): p. 787-799.

10. Holford, i.C.R., r.W.M. Wedderburn, and g.E.G. Mattingly, *A langmuir two-surface equation as a model for phosphate adsorption by soils.* Journal of Soil Science, 1974. **25**(2): p. 242-255.

11. Horta, C., et al., *Phosphorus sorption and desorption properties of soils developed on basic rocks under a subhumid Mediterranean climate.* Soil Use and Management, 2013. **29**: p. 15-23.

12. Huang, Q., W. Liang, and P. Cai, *Adsorption, desorption and activities of acid phosphatase on various colloidal particles from an Ultisol.* Colloids and surfaces B: Biointerfaces, 2005. **45**(3-4): p. 209-214.

13. Janardhanan, L. and S.H. Daroub, *Phosphorus Sorption in Organic Soils in South Florida.* Soil Science Society of America Journal, 2010. **74**(5): p. 1597-1597.

14. Kolahchi, Z. and M. Jalali, *Phosphorus Movement and Retention by Two Calcareous Soils.* Soil and Sediment Contamination: An International Journal, 2013. **22**(1): p. 21-38.

15. Pal, S.K., *Phosphorus sorption-desorption characteristics of soils under different land use patterns of eastern India.* Archives of Agronomy and Soil Science, 2011. **57**(4): p. 365-376.

16. Sakadevan, K. and H.J. Bavor, *Phosphate adsorption characteristics of soils, slags and zeolite to be used as substrates in constructed wetland systems.* Water Research, 1998. **32**(2): p. 393-399.

17. Sanyal, S.K., P.Y. Chan, and S.K. De Datta, *Phosphate Sorption-Desorption Behavior of Some Acidic Soils of South and Southeast Asia.* Soil Science Society of America Journal, 1993. **57**(4): p. 937-937.

18. Sato, S. and N.B. Comerford, *Influence of soil pH on inorganic phosphorus sorption and desorption in a humid Brazilian Ultisol.* Revista Brasileira de Ciencia do Solo, 2005. **29**(5): p. 685-694.

19. Shirvani, M., et al., *Land-Use Conversion Effects on Phosphate Sorption Characteristics in Soils of Forest and Rangeland Sites from Zagros Area, Western Iran.* Arid Land Research and Management, 2010. **24**(919557984): p. 223-237.

20. Singh, B.R., et al., *Phosphorus fractionation and sorption in P-enriched soils of Norway.* Nutrient Cycling in Agroecosystems, 2005. **73**(2-3): p. 245-256.

21. Singh, V., N.S. Dhillon, and B.S. Brar, *Influence of long-term use of fertilizers and farmyard manure on the adsorption-desorption behaviour and bioavailability of phosphorus in soils.* Nutrient Cycling in Agroecosystems, 2006. **75**(1-3): p. 67-78.

22. Villapando, R.R. and D.a. Graetz, *Phosphorus Sorption and Desorption Properties of the Spodic Horizon from Selected Florida Spodosols.* Soil Science Society of America Journal, 2001. **65**(2): p. 331-331.

23. Wisawapipat, W., et al., *Phosphate sorption and desorption by Thai upland soils.* Geoderma, 2009. **153**(3-4): p. 408-415.

24. Xu, D., et al., *Studies on the phosphorus sorption capacity of substrates used in constructed wetland systems.* Chemosphere, 2006. **63**(2): p. 344-352.

25. Zafar, M., et al., *Phosphorus seasonal sorption-desorption kinetics in suspended sediment in response to land use and management in the Guapore catchment, Southern Brazil.* Environ Monit Assess, 2016. **188**(11): p. 643.

26. Zhou, M. and Y. Li, *Phosphorus-Sorption Characteristics of Calcareous Soils and Limestone from the Southern Everglades and Adjacent Farmlands.* Soil Science Society of America Journal, 2001. **65**(5): p. 1404-1404.

27. Zou, P., J. Fu, and Z. Cao, *Chronosequence of paddy soils and phosphorus sorption-desorption properties.* Journal of Soils and Sediments, 2011. **11**(2): p. 249-259.

28. Hinsinger, P., *Bioavailibility of soil inorganic P in the rhizosphere as effected by root-induced chemical changes: A review.* Plant and Soil, 2001. **237**: p. 173-195.

29. Giesler, R., et al., *Phosphate Sorption in Aluminum- and Iron-Rich Humus Soils.* Soil Science Society of America Journal, 2005. **69**: p. 77-86.

30. Penn, C.J., G.L. Mullins, and L.W. Zelazny, *Mineralogy in Relation to Phosphorus Sorption and Dissolved Phosphorus Losses in Runoff.* Soil Science Society of America Journal, 2005. **69**(5): p. 1532-1532.

31. Barros, N.F., et al., *Phosphorus sorption, desorption and resorption by soils of the Brazilian Cerrado supporting eucalypt.* Biomass and Bioenergy, 2005. **28**(2): p. 229-236.

32. Lair, G.J., et al., *Phosphorus sorption-desorption in alluvial soils of a young weathering sequence at the Danube River.* Geoderma, 2009. **149**(1-2): p. 39-44.

33. Borggaard, O.K., et al., *Influence of humic substances on phosphate adsorption by aluminium and iron oxides.* Geoderma, 2005. **127**(3-4 SPEC. ISS.): p. 270-279.

34. D'Angelo, E.M., *Phosphorus sorption capacity and exchange by soils from mitigated and late successional bottomland forest wetlands.* Wetlands, 2005. **25**(2): p. 297-305.

35. Lilienfein, J., et al., *Adsorption of dissolved organic and inorganic phosphorus in soils of a weathering chronosequence.* Soil Science Society of America Journal, 2004. **68**(2): p. 620-620.

36. Schreeg, L.A., M.C. Mack, and B.L. Turner, *Leaf litter inputs decrease phosphate sorption in a strongly weathered tropical soil over two time scales.* Biogeochemistry, 2013. **113**(1-3): p. 507-524.

37. Afif, E., V. Barrón, and J. Torrent, *Organic matter delays but does not prevent phosphate sorption by cerrado soils from Brazil.* Soil Science, 1995. **159**(3): p. 207-211.